

Hadroproduction of D and B mesons in a massive VFNS

B. A. Kniehl, G. Kramer, I. Schienbein* and H. Spiesberger†

**II. Institut für Theoretische Physik, Universität Hamburg, Luruper Chaussee 149,
22761 Hamburg, Germany*

†Institut für Physik, Johannes-Gutenberg-Universität, Staudinger Weg 7, 55099 Mainz, Germany

Abstract. We present a calculation of the next-to-leading order cross section for the inclusive hadroproduction of D and B mesons as a function of the transverse momentum and the rapidity in a massive variable flavor number scheme. We compare our numerical results with recent data from the CDF Collaboration at the Fermilab Tevatron for the production of D^0 , D^{*+} , D^+ , and D_s^+ mesons at center-of-mass energy $\sqrt{S} = 1.96$ TeV and find reasonably good agreement with the measured cross sections.

Keywords: QCD, Heavy Quarks, Heavy Mesons, Heavy Flavor Schemes

PACS: 12.38.Bx, 12.39.St, 13.85.Ni, 14.40.Lb

Various approaches for next-to-leading order (NLO) calculations in perturbative QCD have been applied to one-particle inclusive hadroproduction of D or B mesons. For definiteness, we shall consider here D mesons. However, all results can easily be carried over to any other heavy-flavored hadron.

A basic approach is the fixed flavor number scheme (FFNS) [1], in which the number of active flavors in the initial state is fixed to $n_f = 3$ and the charm quark appears only in the final state. The charm mass m is explicitly taken into account together with the transverse momentum p_T of the observed meson. In this scheme the charm mass acts as a cutoff for the initial- and final-state collinear singularities and collinear logarithms $\ln(p_T^2/m^2)$ are kept in the hard scattering cross sections. However, for $p_T \gg m$, these logarithms become large and spoil the convergence of the perturbation series.

Therefore, in the regime $p_T \gg m$, it is more appropriate to treat charm quarks like massless partons and to absorb the collinear logarithms into scale dependent parton distribution functions (PDFs) and fragmentation functions (FFs). As is well-known, by this procedure the large logarithms $\ln(p_T^2/m^2)$ are summed via the DGLAP evolution equations and the hard scattering cross sections are finite (infrared safe) in the limit $m \rightarrow 0$. If the power-like charm mass terms $\mathcal{O}(m^2/p_T^2)$ are neglected this is just the conventional parton model or zero-mass variable flavor number scheme (ZM-VFNS). Usually, in the ZM-VFNS the charm mass is neglected from the beginning and the collinear singularities appear in dimensional regularization as poles in ϵ where $d = 4 - 2\epsilon$ is the number of space-time dimensions. Conventionally, these poles are removed in the modified-minimal-subtraction (\overline{MS}) scheme. If, on the other hand, the collinear singularities have been regularized with help of a mass m it is necessary also to subtract finite terms along with the collinear logarithms $\ln m^2$ in order to recover the hard scattering cross sections in the \overline{MS} scheme.

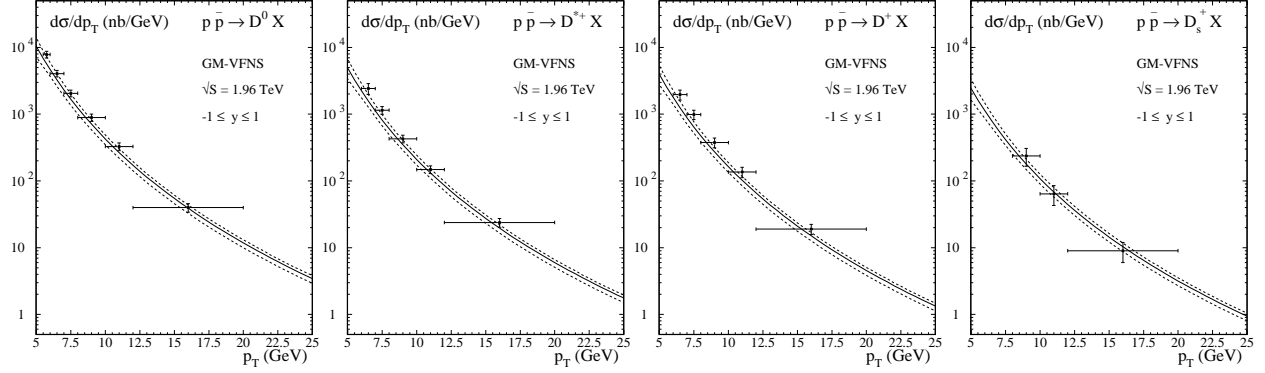


FIGURE 1. QCD predictions for one-particle inclusive production of charmed mesons, $X_c = D^0, D^{*+}, D^+, D_s^+$, at the Tevatron Run II. In each case, the results are shown for the average of the observed meson with its antiparticle $(X_c + \bar{X}_c)/2$. The solid lines have been obtained with $\mu_R = \mu_F = \mu_F' = m_T$. The upper and lower dashed curves represent the maximum and minimum cross sections found by varying μ_R , μ_F , and μ_F' independently within a factor of 2 up and down relative to the central values while keeping their ratios $0.5 \leq \mu_F/\mu_R, \mu_F'/\mu_R, \mu_F/\mu_F' \leq 2$. CDF data [9] are shown for comparison.

On top of these two basic approaches, schemes have been devised which combine the two features, non-zero charm mass and resummation of $\ln(p_T^2/m^2)$ -terms. One such scheme, which has been applied already to inclusive charmed meson production for the Tevatron experiment is the so-called fixed-order next-to-leading-logarithm (FONLL) scheme. This scheme smoothly interpolates between the traditional cross section in the FFNS and a suitably modified cross section in the ZM-VFNS approach with perturbative FFs with the help of a p_T dependent weight function [2, 3]. In both non-zero-charm-mass approaches, FFNS and FONLL, the theoretically calculated cross sections are convoluted with a scale-independent non-perturbative FF extracted from e^+e^- data describing the transition from the produced charm quark to the observed D meson.

Recently, a general mass variable flavor number scheme (GM-VFNS) has been worked out by us [4, 5, 6, 7] which is closely related to the ZM-VFNS, but keeps all m^2/p_T^2 terms in the hard-scattering cross sections in order to achieve better accuracy in the intermediate region $p_T \geq m$. The massive hard scattering cross sections have been constructed in a way that the conventional hard scattering cross sections in the \overline{MS} scheme are recovered in the limit $p_T \rightarrow \infty$ (or $m \rightarrow 0$). The requirement to adjust the massive theory to the ZM-VFNS with \overline{MS} subtraction is necessary since all commonly used PDFs and FFs for heavy flavors are defined in this particular scheme. In this sense this subtraction scheme is a consistent extension of the conventional ZM-VFNS for including charm-quark mass effects. It should be noted that our implementation of a GM-VFNS is similar to the ACOT scheme which has been extended to 1-particle inclusive production of B mesons a few years ago [8]. There are small differences concerning the collinear subtraction terms [5]. Further, in [8], the resummation of the final state collinear logarithms has been performed only to leading logarithmic accuracy.

To calculate the cross section $d^2\sigma/dp_T dy$ for the reactions $p + \bar{p} \rightarrow D + X$, FFs are needed which describe the fragmentation of the charm quarks, the light quarks, and the gluon into the observed D mesons. Fragmentation functions for the D^* meson

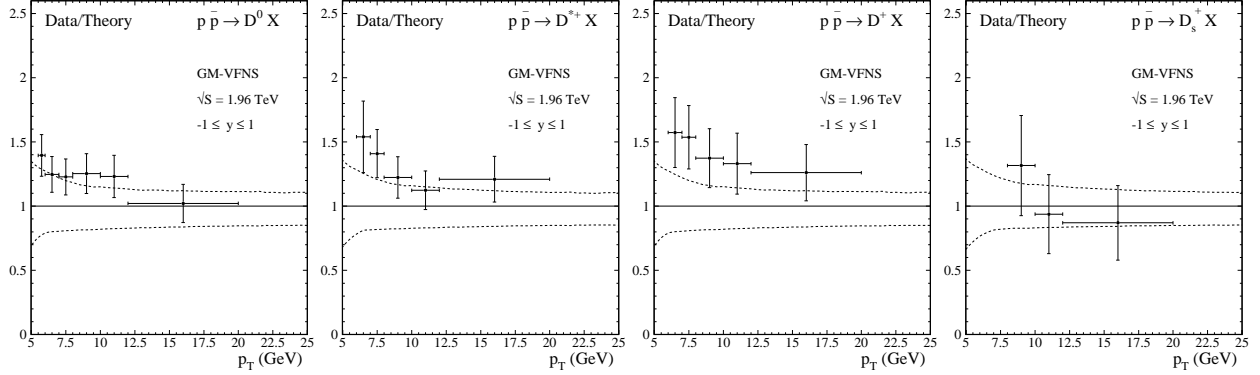


FIGURE 2. Ratios of experimental results and our central theoretical predictions (solid lines in Fig. 1). In addition, the theoretical uncertainty bands are shown, obtained as the ratio of the upper (lower) QCD prediction and the central curve.

have been extracted at leading and next-to-leading order already some time ago [10], using experimental data from the OPAL [11] and ALEPH [12] collaborations at LEP1. Recently, using the same procedure as in [10], also the FFs for $X_c = D^0, D^+, D_s^+, \Lambda_c$ have been determined [13] using OPAL data for $e^+e^- \rightarrow X_c + X$ [14]. In Refs. [10, 13] the fits for the X_c FFs have been performed using a starting scale $\mu_0 = 2m$ for the gluon and the u, d, s and c quarks and their antiquarks, while $\mu_0 = 2m_b$ ($m_b = 5$ GeV) was chosen for the FFs of the bottom quark and antiquark. The FFs of the gluon and the first three flavors were assumed to be zero at this μ_0 . At larger scale μ , these FFs are generated through the usual DGLAP evolution. Since the effect of the gluon FF is important at Tevatron energies as was found for D^* production in [4] we decided to repeat the fits for the X_c FFs with the lower starting scales $\mu_0 = m$ and $\mu_0 = m_b$, respectively. This changes the FFs of the c quark only marginally but has a sizable effect on the gluon FF. The details of these new FFs will be presented elsewhere [15].

Next we show our predictions for the cross sections $d\sigma/dp_T$ for D^0, D^{*+}, D^+ and D_s^+ production obtained in the GM-VFNS. For a comparison with the ZM-VFNS we refer to Ref. [16]. The partonic cross sections are convoluted with the (anti-)proton PDFs and the FFs for $c \rightarrow X_c$, $u, d, s \rightarrow X_c$ and $g \rightarrow X_c$. We use CTEQ6M PDFs [17] and the FF sets for D^0, D^{*+}, D^+ and D_s^+ from [15].¹ Results are shown for the average of the observed X_c mesons with their antiparticles. We consider $d\sigma/dp_T$ at $\sqrt{S} = 1.96$ TeV as a function of p_T with y integrated over the range $-1.0 < y < 1.0$. For the charm mass we take $m = 1.5$ GeV and evaluate $\alpha_s^{(n_f)}(\mu_R)$ with $n_f = 4$ and scale parameter $\Lambda_{\overline{MS}}^{(4)} = 328$ MeV, corresponding to $\alpha_s^{(5)}(m_Z) = 0.1181$. The results are presented in Figs. 1 and 2. The solid lines correspond to the central scale choice $\mu_R = \mu_F = \mu'_F = m_T = (p_T^2 + m^2)^{1/2}$, where μ_R is the renormalization, μ_F the initial-state and μ'_F the final-state factorization scale, respectively. To investigate the scale

¹ It should be noted that the results presented at the DIS05 have been obtained with the FFs from [10, 13].

variation of our predictions, we independently vary the renormalization and factorization scales by a factor of two: $0.5 \leq \mu_R/m_T, \mu_F/m_T, \mu'_F/m_T \leq 2$ while keeping their ratios $0.5 \leq \mu_F/\mu_R, \mu'_F/\mu_R, \mu_F/\mu'_F \leq 2$ [16]. Our theoretical results are compared with the experimental data from CDF [9]. As can be seen, the data are in good agreement with the upper curve of the uncertainty band whereas they are a factor of about 1.5(1.2) above our central prediction at low(high) p_T .

Residual sources of theoretical uncertainty include the variations of the charm mass and the assumed PDF and FF sets. A variation of the value of the charm-quark mass does not contribute much to the theoretical uncertainty. Also the use of other up-to-date NLO proton PDF sets produces only minor differences. Concerning the choice of the NLO FF sets we obtain results reduced by a factor of 1.2–1.3 when we use the NLO sets obtained by fitting with the initial scale choice $\mu_0 = 2m, 2m_b$.

In conclusion, we have presented a NLO perturbative QCD calculation of D meson production at the Tevatron in a GM-VFNS [4, 5] which provides the best description of these experimental results obtained so far. It completes earlier work in this scheme on D meson production in $\gamma\gamma$ and γp collisions [18]. This approach will be applied next to B meson production at the Tevatron. Furthermore, it is planned to extend this scheme to heavy meson production in deep inelastic scattering.

ACKNOWLEDGMENTS

This work was supported in part by the Bundesministerium für Bildung und Forschung through Grant No. 05 HT4GUA/4. The work of I. S. was supported by DESY.

REFERENCES

1. P. Nason, S. Dawson, and R. K. Ellis, *Nucl. Phys.*, **B303**, 607 (1988); **B327**, 49 (1989); **B335**, 260(E) (1990); W. Beenakker, H. Kuijf, W. L. van Neerven, and J. Smith, *Phys. Rev.*, **D40**, 54 (1989); W. Beenakker, W. L. van Neerven, R. Meng, G. A. Schuler, and J. Smith, *Nucl. Phys.*, **B351**, 507 (1991); I. Bojak, and M. Stratmann, *Phys. Rev.*, **D67**, 034010 (2003).
2. M. Cacciari, M. Greco, and P. Nason, *JHEP*, **05**, 007 (1998).
3. M. Cacciari, and P. Nason, *JHEP*, **09**, 006 (2003).
4. B. A. Kniehl, G. Kramer, I. Schienbein, and H. Spiesberger, *Phys. Rev.*, **D71**, 014018 (2005).
5. B. A. Kniehl, G. Kramer, I. Schienbein, and H. Spiesberger, *Eur. Phys. J.*, **C41**, 199 (2005).
6. I. Schienbein, hep-ph/0408036.
7. I. Schienbein, Open heavy-flavour photoproduction at NLO, Proceedings of the Ringberg Workshop, *New Trends in HERA Physics 2003*, edited by G. Grindhammer, B. A. Kniehl, G. Kramer and W. Ochs, World Scientific, 2004, p. 197.
8. F. I. Olness, R. J. Scalise, and W.-K. Tung, *Phys. Rev.*, **D59**, 014506 (1999).
9. D. Acosta, et al., *Phys. Rev. Lett.*, **91**, 241804 (2003).
10. J. Binnewies, B. A. Kniehl, and G. Kramer, *Phys. Rev.*, **D58**, 014014 (1998).
11. K. Ackerstaff, et al., *Eur. Phys. J.*, **C1**, 439 (1998).
12. R. Barate, et al., *Eur. Phys. J.*, **C16**, 597 (2000).
13. B. A. Kniehl, and G. Kramer, *Phys. Rev.*, **D71**, 094013 (2005).
14. G. Alexander, et al., *Z. Phys.*, **C72**, 1 (1996).
15. B. A. Kniehl, G. Kramer, I. Schienbein, and H. Spiesberger, in preparation.
16. See the Proceedings of the HERA-LHC Workshop.
17. J. Pumplin, et al., *JHEP*, **07**, 012 (2002).
18. G. Kramer, and H. Spiesberger, *Eur. Phys. J.*, **C22**, 289 (2001); **C28**, 495 (2003); **C38**, 309 (2004).